www.rericjournal.ait.ac.th

Continuous Ethyl Ester Production in a High-Performance Rotor Reactor at 3:1 Molar Ratio using Response Surface Methodology

Wuttisan Khiowthong * and Prachasanti Thaiyasuit *, [1]

ARTICLE INFO

Article history:
Received 30 April 2023
Received in revised form
13 August 2023
Accepted 21 August 2023

Keywords:
Biodiesel
Bumpy surface rotor reactor
Optimal conditions
Resultant velocity
Severe cavitation

ABSTRACT

The aim of this study was to investigate the optimal conditions for continuous ethyl ester production and to validate the values of the parameters influencing the production performance. Experiments were performed at a 3:1 ethanol-to-oil molar ratio using a high-performance rotor reactor equipped with a rotor of 27.6 A_F% (holes surface per rotor surface). Response surface methodology using a 3-variable 5-level central composite design was applied to vary over the range of 2160–3840 rpm rotor speed, 0.33-1.73 wt% potassium hydroxide [KOH], and 2.32–5.68 L/min flow rate. The three-parameters identified were resultant velocity (V_R), Cavitation number, and Reynolds number. Production performances were yield conversion and specific energy consumption (SEC). The regression model predicted optimal conditions of 3000 rpm rotor speed, 1.170 wt% [KOH], and 5.68 L/min flow rate with ethyl ester content (C_{EE}) of 98.84 wt%, and the actual testing showed an average C_{EE} of 98.11 wt% The V_R of 15.732 m/s resulted in a 4449.74 Reynolds number, with a Cavitation number 0.732 showing severe cavitation and turbulence to generate a 97.98 wt% yield conversion using only 0.00459 kW-h/kg of SEC.

1. INTRODUCTION

In the new era, there was a growing interest in using clean fuels such as ethyl ester (EE) in biodiesel to protect the surroundings despite methyl ester (ME) being the first ester to be introduced. Alternative factors of clean EE were attracted by utilizing ethanol instead of methanol. From an environmental point of view, EE utilization had been found to be more advantageous than ME utilization [1]. Bioethanol was a renewable energy source that could be produced from agricultural resources such as sugarcane and cassava, being completely independent of importing petroleum-based alcohol [2]. The choice of ethanol was based on dissolution properties. Ethanol was a good solvent, with a high solubility capacity for oils and was usually used as a suitable reactant for the transesterification of waste cooking oil (WCO). The base-catalyzed formation of EE had more complexity than the formation of ME. Producing EE had been shown to be considerably interesting because the extra carbon atom provided by ethanol increased the heat content [3]. The synthesis of biodiesel progressed via the transesterification reaction, where ethanol promoted a more stable dispersion among the products, impedes the layer separation and increased the reaction time of the process, which lowers the biodiesel quality [4]. The process produced EE by the reaction of ethanol with vegetable oil, which required high energy consumption for excitation, and the product content of EE had been discovered to be highly dependent on the reaction temperature, water content, free fatty acid (FFA), oil type, initial ethanol: oil molar ratio, and catalyst loading [5].

The EE content had been found to vary with the quantity of water in the reactants. If the water content was high, it affected stable emulsions formed during the process. The separation of EE from the product was made more difficult by this fact [6].

The type of catalyst applied depended on FFA and the water content in the precursor. FFA and water were responsible for the saponification reaction and soap formation [7]. The preparation of the reactants should deal with both water and FFA. All FFA and water could be reduced by using a two-step process of biodiesel production with an acid catalyst, but this reaction rate was slow and receives a lower EE than base-catalyst reaction. However, the large amount FFA and water was the main reason for using a higher amount of base catalyst. The mixture of water, oil, and base catalyst at high temperature led to the activation of the saponification reaction which decreased the EE and created difficulties in phase separation. The optimal catalyst loading amount depended on the kind, quality of oil, and type of base catalyst.

The reaction rate and EE content were dependent on the initial ethanol: oil molar ratio. Since the reaction was reversible, an increase in the molar ratio shifted the reaction equilibrium toward EE formation, but using a lower molar ratio and a low catalyst loading made the production mixture non-separable [8]. On the other

* Department of Mechanical Engineering, Faculty of Engineering, Ubon Ratchathani University, Warin Chamrap, Ubonratchathani 34190, Thailand.

[1]Corresponding author:
Email: prachasanti.t@ubu.ac.th

hand, using a molar ratio higher than 12:1 the glycerol separation was difficult because the excess ethanol would keep the glycerol in the remaining EE phase. The initial molar ratio must always be optimized. For mechanical stirring, the optimal molar ratio depends on the temperature, type of oil, catalyst type, and loading.

Generally, biodiesel was produced by means of a transesterification reaction in which triglycerides (TG) react with alcohol to form esters and glycerol which was reversible. The process consisted of three sequences, namely the reaction of TG with alcohol to form diglycerides (DG) and a first ester, the reaction of DG with the alcohol to form monoglycerides (MG), and the reaction of a second ester and MG with the alcohol to form a third ester and glycerol, receiving an ester from each glyceride in each step. In practice, this usually increased the molar ratio to 6:1, which raised the yield, and forced the equilibrium to advance toward the product side [9].

To reduce costs, WCO had become more attractive for alternative materials. After filtering out the suspension and removing the moisture, the treated WCO had properties close to those of refined oil. It could be used to produce biodiesel via a transesterification process [10]. The low cost of raw materials, including high energy efficiency, was the main reason for reducing the total cost of biodiesel production [11].

These possibilities improved the reaction of EE production by using a high-performance reactor, increasing the EE content and decreasing the reaction time to reduce the reverse reaction. Efficiency was improved by using optimal technologies for biodiesel production. Technologies commonly used biodiesel production were mechanical stirrer (MS), microwave (MW), ultrasonic cavitation (UC), and hydrodynamic cavitation (HC) [12]. The MS reactor via the transesterification process had reversal limitations due to the discontinuity of product separation, which did not benefit from continuous production.

Microwave technology had a similar effect in terms of increasing the rate of reaction. The MW reactor delivered energy directly to the precursor, heat transfer was more effective than a conventional heater, and the reaction could be completed in a short time. Continuous EE of waste fried palm oil gave a yield conversion of over 97wt % in a residence time of 30 s [13]. A comparison was made between the base-catalyzed EE production of esterified crude palm oil under MW and MS heating at 70˚C. The high EE content was produced by MW for 5 min, while MS heating required 1 h to achieve the same EE content [14].

UC was typically used to enhance the reaction rate of a homogeneously base-catalyzed EE production which results in higher EE content in a shorter retention time. UC was economically more beneficial than MS due to lower energy consumption and shorter separation times. So this UC could be effectively applied for continuous production [15]. Under optimal conditions, ultrasound-assisted base-catalyzed EE production of triolein produced 98 wt% EE content in less than 20 min, compared to MS, which produced only 90 wt% EE content in a long time of 25 min [16].

Several researchers had commended HC technology for its many benefits compared to other conventional techniques. HC reactors had advantages over their classic batch chemical processes, such as them being the most energy efficient in generating HC, high flexibility, simple setup, easy adjustment, low chemical consumption, and time saving [17]. Furthermore, due to its configuration, HC could produce cavitation of greater intensity. Better cavitation results could be achieved, depending only on the geometry of HC devices [18]. Cavitation could be generated by both static and dynamic system types. For a static system using high power consumption, the flow velocity was forced to produce cavitation by reducing the static pressure as the fluid passed through the small static parts. Static HC technique when used with the synthesized catalyzer exhibited resulting energy savings coherency, time savings, and building the operation more resource-efficient [19]. For dynamic systems, the rotor reactor provided high mixing due to the occupancy of high shear and speed but used lower power consumption to develop mixing of the precursor, generated turbulent flow, and reduced static pressure to generate HC [20]. HC was a phenomenon that occurred during the internal flow process of rotating machinery. HC occurred when the liquid was subjected to a pressure drop, which was equal to or lower than the vapor pressure at a given temperature [21]. The formation of bubbles had a potential energy. The potential energy released by bubble formation on their volume and bubble pressure [22] could be used to determine the specific properties of the surrounding liquid [23]. The collapse of bubbles generated a lot of energy in the form of shock waves [24], characterized by the collapse of bubbles in fluid flow and the release of heat from the explosive at high temperatures [25].

Efforts have been made to find new high efficiency reactors that could save more energy and time. Mass transfer efficiency was a major design limitation in the transesterification process. Although many reactors generated a vigorously mixed mixture, they still consumed high energy [26]. WCO had been used in conjunction with a rotor reactor to study HC [27]. In the HC reactor, a rotor part was built as a rigid metal cylinder with holes on its surface, and cavitation regions were established inside and around the holes due to the high-speed of rotation. The rotation of the rotor reactor caused a pressure drop in the system, requiring the use of additional feed pumps to increase the compensating pressure in the reactor to force the reactants to flow in the operating region. Recently, researchers have improved the system by increasing the energy efficiency using a compact reactor equipped with a feeder pump [28].

The modern reactor rotor-stator type was designed [29]. The reactor was equipped with a stainless steel rotor having 40 holes on the rotor surface and driven by an electric motor with a power of 75 W and a rotational speed of 3200 rpm. The dimensions of the stainless steel rotor were 90 mm in diameter, 80 mm in length, 4 mm in hole diameter, and 97 mm in stator diameter. Applied to the production of ME, a maximum yield conversion

of 89.11 wt% was obtained to support the production under optimal conditions of methanol to oil molar ratio of 8.36:1, KOH concentration of 0.94 wt%, and reaction time of 63.88 s [30].

The latest innovation, the rotor-stator reactor, was developed and equipped with rotors of 3D printed type and stainless steel type with 80 holes on the rotor surface, driven by a 3.7 kW electric motor with a rotational speed of 3000 rpm. The rotor dimensions were 60 mm in diameter and 46 mm in length, with an optimal hole diameter of 6.4 mm and a depth of 6.2 mm with a stator diameter of 80 mm. To produce ME in a two-step production process the ME purities of 99.16 wt% with 3D printed rotors and 99.22 wt% with a stainless steel rotor were respectively received. The two-stage production process consumed 0.049 kW-h/L of low energy for the entire complete continuous process [31].

In this article, all continuous biodiesel production was performed using a bumpy surface rotor reactor (BSRR) equipped with a rotor having a total hole surface area per rotor surface area of 27.6 % and a molar ratio of alcohol to oil of 3:1. The experiment was aided by the application of a three-variable, five-level response surface methodology (RSM) and a central composite design (CCD).

The BSRR was tested for running to indicate a zero code in the CCD. Instruments such as thermocouples, pressure transmitters, and data loggers were calibrated. It was found that the vapor pressure within the BSRR of ethanol was one-half lower than that of methanol at room temperature. Under this limitation, biodiesel production using ethanol was generally less effective than using methanol.

The twenty (20) experiments were designed using CCD, and RSM was used to analyze the experiment data. The regression RSM model was developed and used to predict the optimal conditions and ethyl ester (EE) content. Supporting the optimal conditions is the first objective of the experiment. Optimal conditions were set to validate EE content and production performance, such as yield conversion and specific energy consumption. Significant parameter effects were validated for V_X conversion from flow rate combined with V_Y conversion from rotor speed to resultant velocity (V_R), with the physical properties of the precursor, such as density and viscosity, being tested. Temperature and pressure were validated to calculate the vapor pressure (P_V) at the internal reference point of the reactor at time intervals ranging from 0-60 s. Physical property values, V_R and P_V, were used to calculate the cavitation number and Reynolds number in response to production performance and were described in detail. Validation of the parameter values influencing the production performance answering the second objective of the experiment.

The results of the relationship between parameters and performance for EE production were compared to the continuous ME production [32] that had been fully successful.

2. MATERIALS AND METHODS

2.1 Materials

WCO from refined palm olein was purchased from a fried chicken shop near Ubon Ratchathani University, Thailand. It was filtered through a No. 30 mesh sieve and dehumidified by boiling at 110℃ for 1 h. The treated WCO had an AV of 2.13 mg KOH/g and 1.07 FFA $_{Oleic}$ %, as shown in Equation 1.

$$FFA_{Oleic} = \frac{AV}{1.99} \quad (1)$$

where FFA $_{Oleic}$ is the percentage of free fatty acid (FFA%)[A], and AV is the acid value (mg KOH/g)[B] in accordance with EN 14104 standard. The molecular weight of WCO (MW_{WCO})[C] is 846.81 g/mol and molecular weight of FFA (MW_{FFA})[D] is 271.66 g/mol [32]. A, B, C and D were tested by the Scientific Instrument Center of Ubon Ratchathani University (SICUBU). Commercial grade (99.9 vol%) was used for ethanol and methanol. Industrial grade (90 wt%) was used for KOH.

2.2 Rotor Reactor Experimental Setup

The experimental setup for continuous biodiesel production via hydrodynamic cavitation process using BSRR was shown in Figure 1. BSRR was an important part of the equipment available for continuous EE production via the transesterification process. Detail of dimensions were described in a previous paper [32] on the ME production.

The BSRR was equipped with a hollow rotor having a diameter of 100.2 mm and a length of 264.0 mm. The stator was a stationary part of the reactor. Its dimensions were 109.2 mm inner diameter and 127.0 mm outer diameter. All parts were made of high-carbon steel resistant to base catalysts. The rotor surface was drilled with 120 cylindrical shape holes dimensions of 9.0 mm diameter and 4.5 mm depth and an area fraction of 27.6 A_F%. The relation of A_F was shown in Equation 2 and the BSRR installed location was shown in Figure 1. Digital flow meter model OGM-D-25 flow range (0-200LPM) ± 0.5%. An electric induction motor (model: SF-JR 4kW 2P 3 phase) was used to drive the BSRR with a pulley driving ratio of 4:1. To adjust the rotor speed, an inverter (model: VB5N 43P7G-S/45P5P) was used to control the motor speed. The Inverter controller adjusted the frequency at a nominal speed of ± 10 rpm. The energy consumption was measured using a three-phase LCD Watt-hour meter (model: DTM 0243) IEC62053-21 accuracy class 1.0. HC validation, temperature, and pressure were measured using 5 sets of thermocouple: TC17 (-50…+250°C) type K with accuracy ±0.01 °C and 5 sets of pressure transmitter: PT301 (0...6 bar) accuracy ±0.05%FS. All data were recorded using a Data Logger model DL-2 Signal 4-20 mA 12 Chanel Linear current in range -20... +20 mA.

$$A_F = \frac{a_{Holes}}{a_{Rotor\ Surface}} \times 100 \quad (2)$$

where A_F is the percentage of the total holes surface area (a_{Holes}) to the rotor surface area ($a_{Rotor\ Surface}$) [32].

2.3 Experimental Procedure of Rotor Reactor

Experimental procedures for continuous EE production using the BSRR, referring to the BSRR setup in Figure 1, could be described in the following order:

The treated WCO was stored in the WCO tank (T_1) with a capacity of 200 L and a magnet pump (P_1, SANSO, model: PMD-371) at a flow of 25 L/min, a stainless ball valve and digital flow meter regulating the flow direction pass through the pipe diameter of 19.0 mm.

In preparing the KOH solution, the required ratios of solution were predetermined by dissolving the KOH in alcohol in an external mixing bin and loading it into the tank (T_2) with a capacity of 10 L. The top of the T_2 was equipped with an agitator and a dosing pump (P_2, EMEC model: AMSMF 0720 FP) to mix and feed the solution by adjusting the flow rate up to a maximum of 20 L/h.

WCO (T_1) and KOH solution (T_2) were pumped and injected through check valves and flowed into the Y-joint inlet, mixing in a 1:3 molar ratio. The reactant was injected until it completely filled the reactor capacity. The vent valve was opened until the BSRR was emptied of air.

In the next step, the inverter switch was turned on and the frequency was adjusted to calibrate the rotor speed. The data logger was turned on. The inverter start switch was pressed to drive the reactor as per the set speed. The precursor inside the reactor was rotated at high velocity to reach equilibrium reaction within 30 s and retain the samples.

The BSRR ran continuously for 60 s and the data logger recorded temperature and pressure inside the BSRR every 2 s. At 30 s, the sampling valve was opened, and the products were collected as samples of 100 ml for each condition. At 60 s, the net energy consumption was recorded, and the total mass of biodiesel was collected. All products were cooled down in cold water to stop the reaction immediately. Glycerol was separated by gravity after 4 h into neat biodiesel without cleaning with warm water. This was caused by the use of an alcohol: oil molar ratio of 3:1 and the low concentration of KOH used.

The predicted optimal conditions were repeated in the experiments three times to determine the actual ester content. MG, DG, TG, and total glycerol were analyzed following the EN14105 standard. Ester content analysis was performed using Gas-chromatography (GC) and flame ionization detection (FID) to investigate the neat biodiesel compositions following the EN14103 standard.

CLARUS GC680 was equipped with an automatic injector, FID, and Elite-5 capillary column Perkin Elmer PN.no. 9316086 (length 30 m, $Ø_{ID}$ 0.32 mm, film thickness 0.25 µm) was used at a temperature in the range of -60°C to 330/350°C. The stationary phase was methylpolysiloxane. Methyl nonadecanoate ($C_{20}H_{40}O_2$) was used as an internal standard. A 1 µL sample was injected via a sample at an oven temperature of 195°C. After an isothermal period of 5 min, the GC oven was heated to 240°C at 5°C/min and held for 12 min. The GC oven was then heated to 290°C at 30°C/min and held for 5 min. Helium was used as the carrier gas at a flow rate of 2 mL/min, measured at 20°C. Air and hydrogen were used at a flow rate of 450 ml/min and 45 ml/min for the flame.

All properties of neat biodiesel were analyzed based on the EN 14214 standard by the SICUBU.

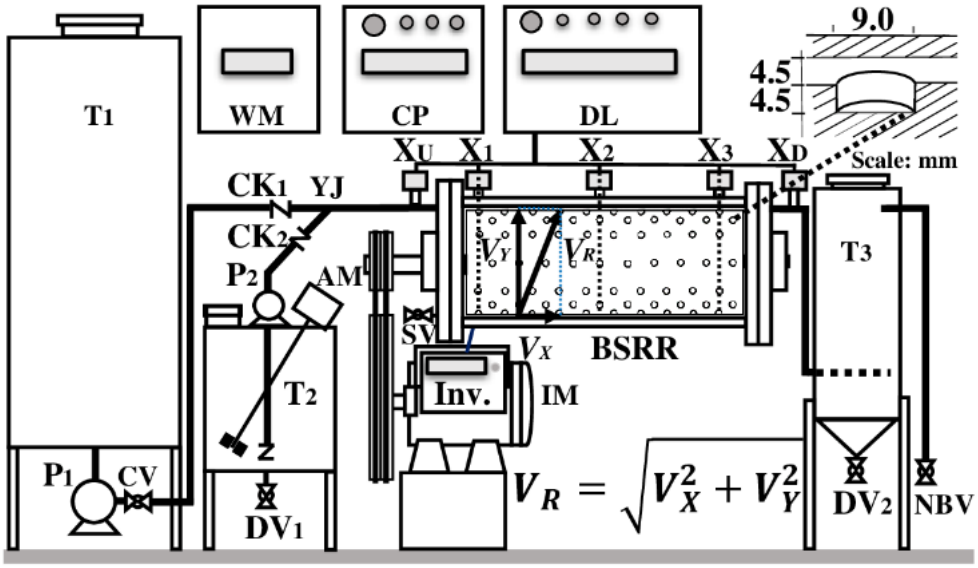

Fig.1. Schematic diagram of the experimental setup.

(T_1: WCO tank, T_2: alcohol tank, T_3: glycerol separation tank, P_1: WCO pump, P_2: alcohol dosing pump, AM: agitator motor, IM: induction motor, CV: flow rate control meter, DV: drain valve, SV: sampling valve, NBV: neat biodiesel valve, CK: check valve, YJ: Y joint, WM: Watt hour meter, Con.: control panel, DL: data logger recorded 5 sets of TC17 and 5 sets of PT301, Inv.: inverter controller, V_X: the steady flow velocity (V_{XU} and V_{XD} are V_X at inlet and outlet, $V_{X1,X2,X3}$ are V_X at point 1, 2, and 3), V_Y: the tangent line velocity, and V_R: the resultant velocity)

2.4 Experimental Design

Response surface methodology was used to analyze the fit of the actual experimental conditions to the predicted optimal conditions for purified ethyl ester (EE). A polynomial model with second-order multiple regression analysis was developed and used to predict EE content, including a search for optimal conditions.

In this study, EE content was the response results of three variables: rotor speed of 2160–3840 rpm, KOH concentration [KOH] of 0.33-1.73 wt% and flow rate of 2.32 to 5.68 L/min, which were the best conditions for the search of variation. In the central composite design (CCD), three variables with five levels of -1.68179, -1, 0, +1, and +1.68179 were optimized and the ranges of variables values were shown in Table 1.

Table 1. CCD coded levels with α =1.68179.

Symbol: Variable (Dimension)	Limit value and code level				
	-α	-1	0	1	+α
A: Speed (rpm)	2159	2500	3000	3500	3840
B: [KOH] (wt%)	0.33	0.50	0.75	1.00	1.17
C: Flow rate (L/min)	2.32	3.00	4.00	5.00	5.68

2.5 Dependent Variable Parameters and Performances

The significant parameters in the relational function between the physical variables were investigated and compared with the effects on the dependent variable between continuous ethyl and methyl ester production and their production performances.

2.5.1 Dependent variable

The ethyl and methyl ester content (C_{EE} *and* C_{ME}) were calculated according to Equations 3 and 4, respectively. The variables for ethyl ester content and methyl ester content were defined by the following equations:

$$C_{EE} = \frac{\left[\left(\sum A_{SUM} - \sum A_{ME} - A_{EI} - A_H\right) \times M_{EI} \times 100\right]}{\left(A_{EI} \times M_{SAM}\right)} \quad (3)$$

$$C_{ME} = \frac{\left[\left(\sum A - A_{EI} - A_H\right) \times M_{EI} \times 100\right]}{\left(A_{EI} \times M_{SAM}\right)} \quad (4)$$

where C_{EE} is the ethyl ester content (wt%), C_{ME} is the methyl ester content (wt%), ΣA_{SUM} is the total signal peak area of the total ester, ΣA_{ME} is the total peak area of the methyl ester, A_{EI} is the internal standard peak area, A_H is the peak area of the heptane solution, ΣA is the total peak area, M_{SAM} is the weight of the neat biodiesel sample (mg), and M_{EI} is the weight of the internal standard (mg).

2.5.2 Significant parameters

- The significant parameters were the resultant velocity (V_R), the cavitation number (σ), and the Reynolds number (Re). The most significant parameter was the V_R of the precursor in the spiral flow direction of the cylinder shape holes on the rotor surface, which was described. V_X was the velocity as a function of steady flow rates and V_Y was the velocity as a function of rotor speed. Since the precursor layer on the rotor surface was very thin, V_Z was assumed to be approximately zero. The summation of the x-y direction velocity was combined to become the $V_{R,}$ as shown in Figure 1, and was given by:

$$V_R = \sqrt{V_X^2 + V_Y^2} \quad (5)$$

$$V_x = \frac{Q}{A_{ref}}; \text{and } V_y = \frac{\pi \times \phi_{ID} \times speed}{60}$$

where V_R is the resultant velocity (m/s), V_X is the velocity in the x-direction (m/s), Q is the flow rate (m^3/s), and A_{REF} is the cross-sectional area (m^2) at the reference point (A_{XU}=A_{XD}, A_{X1}=A_{X2}=A_{X3}). V_Y is the velocity on the tangent line of the rotor (m/s), $Ø_{OD}$ is the outer diameter of the rotor (m), and speed is the rotor speed (rpm).

The cavitation number was the second significant parameter that predicted the opportunity to generate cavitation in the rotor reactor. If the σ value was less than 1, then the cavitation was severe. The value of σ based on the measurement condition over the reference point was given by the following equation:

$$\sigma = \frac{P_{REF} - P_{V(T_{REF})}}{\frac{1}{2}\rho V_R^2} \quad (6)$$

Equation 6 was used to determine σ, where T_{REF} and P_{REF} are reference values for temperature (K) and pressure (N/m^2) measuring the flow rate [33] inside the rotor reactor, ρ is the mixture reactant density (kg/m^3), and $P_{V(T\ REF)}$ is the vapor pressure (N/m^2) at T_{REF}.

$$P_{V(T_{REF})} = \left(P_{V,alc} \times X_{alc}\right) + \left(P_{V,WCO} \times X_{WCO}\right) \quad (7)$$

Raoul's Equation 7 was used to determine the total vapor pressure of an alcohol and WCO mixture at the reference temperature ($P_{V,(TREF.)}$) where $P_{V,\ alc.}$ is the P_V of the alcohol (N/m^2) [34], and $P_{V,\ WCO}$ is the P_V of the WCO (N/m^2) which is close to 0 N/m^2 at room temperature [35]. At a molar ratio of 3:1, $X_{\ alc.}$ is the molar fraction of alcohol at 0.75 and X_{WCO} is the molar fraction of WCO at 0.25.

$$P_{V,alc} = 10^{\left(A-\left(\frac{B}{T+C}\right)+5\right)} \quad (8)$$

Antoine's Equation 8 was used to determine the alcohol vapor pressure, where $P_{V,\ alc.}$ is the vapor pressure of methanol or ethanol (N/m^2) and T is the temperature of the alcohol (K). The Antoine equation shows methanol coefficients of A=5.204, B=1581.341, and C= -33.500 using a range T of 288.10 to 356.83K, and ethanol coefficients of A=5.247, B=1598.673, and C= -46.424 using a range T of 292.77 to 366.63K [34].

The third parameter was the Reynolds number (*Re*). *Re* could describe the flow behavior. If a value was less than 2000, it was a laminar flow behavior, if it was greater than 2000 and less than 4000, it was the transition zone of type II flow, and if it was greater than 4000, it was turbulent flow. *Re* could be computed as follows:

$$Re = \frac{\rho V_R D_H}{\mu} \quad (9)$$

$$\nu = \frac{\mu}{\rho}$$

where *Re* is a dimensionless Reynolds number, V_R is the resultant velocity (m/s), ρ is the mixed fluid density (kg/m^3), μ is the dynamic viscosity (Pa·s), ν is the kinematic viscosity (m^2/s), D_H is a characteristic linear dimension (m) exactly equal to the inner diameter of the pipe of the inlet-outlet reactor circular pipes, and the hydraulic diameter ($D_H = D_o$-D_i) is the difference value of D_O (outer diameter) and D_i (inner diameter) used for the annular duct as the outer channel of a rotor in a stator [32].

2.5.3 Performances

The transesterification process was stimulated by HC. The RSM model presented an equation to predict the optimal conditions, and the proposed conditions were validated by repeating them three times. The exact results were used to calculate the yield conversion (*Y*) and specific energy consumption (*SEC*) [32] by:

$$Y = \frac{\dot{M}_{NB} \times 100}{\dot{M}_{WCO}} \quad (10)$$

$$SEC = \frac{\dot{EC}}{\dot{M}_{NB}} \quad (11)$$

where Y is the yield conversion (wt%), $\dot{M}_{NB}$ is the mass flow rate of neat biodiesel (kg/min), $\dot{M}_{WCO}$ is the mass flow rate of WCO (kg/min), *SEC* is the specific energy consumption (kW-h/kg), $\dot{E}C$ is the energy consumption rate (kW-h/min).

3. RESULTS

3.1 Experimental Results

The 20 experiments for the 3 variables (rotor speed, [KOH], and flow rate) were varied over 5 levels of CCD. Table 2 provided a complete description of the C_{EE} results. The RSM model, predictive results and statistical analysis were described in the next section.

3.2 RSM Model of Results and Statistical Analyses

RSM was used to evaluate the fitted regression model for EE production from this continuous process using BSRR.

The regression function was expressed as a second-order polynomial in multiple variables given by the following:

$$C_{EE} = \beta_0 + \beta_1 A + \beta_2 B + \beta_3 C + \beta_4 AB + \beta_5 AC + \beta_6 BC + \beta_7 A^2 + \beta_8 B^2 + \beta_9 C^2 \quad (12)$$

where C_{EE} is the ethyl ester content (wt.%), A is the rotor speed code, B is the KOH concentration code, C is the flow rate code, and β is the fixed coefficient.

The RSM model predicted the results and illustrated the statistical significance of the regression coefficients by *P*-values of less than 0.05, as listed in Table 3. The model still illustrated satisfactory values for the *R-square* (R^2) and the *R-square adjusted* ($R^2_{adjusted}$).

Under the statistical definition, a strong and significant result was obtained for this experiment. Observations were presented in Table 3 to describe each parameter. Significance with a *P*-value less than 0.05 was found in all three variables and could be ordered from highest to lowest level of significance, namely $\beta_2 B$, $\beta_3 C$, and $\beta_1 A$. As a result, the highest level of significance was found for the KOH concentration [KOH] in the coefficient of $\beta_2 B$, which combined with $\beta_4 AB$ and $\beta_6 BC$ had a greater effect on the production of high purity of ethyl ester. Therefore, [KOH] was the most important factor for the production of ethyl ester in this process.

The variance analysis of the RSM model corresponding to the continuous process by Minitab16 was shown in Table 4. The model was considered to analyze the importance of the three independent variables for the statistical response model. The high coefficient of determination R^2 was 0.9969, indicating the acceptance of the model and the ability to fit the actual results well. The adjusted determination coefficient $R^2_{adjusted}$ value of 0.9941 indicates that the RSM model equation yields a confidence value higher than 0.95. The high *F*-Value distribution of 356.44 supported a *P*-Value of 0.000 that was below 0.05 and considered acceptable. In addition, the *P*-Value for Lack-of-Fit was 0.167 higher than 0.05, which illustrated the confidence level of the RSM model. Equation 12 could be used to solve the solution exactly and indicate reasonable consistency in the regression RSM model.

Table 2. Design of experiment and C_{EE}.

Run	*A* (rpm)	*B* (wt%)	*C* (L/min)	C_{EE} (wt%)
1	2500	0.50	3.00	94.832
2	3500	0.50	3.00	96.352
3	2500	1.00	3.00	92.217
4	3500	1.00	3.00	95.898
5	2500	0.50	5.00	94.445
6	3500	0.50	5.00	90.383
7	2500	1.00	5.00	97.796
8	3500	1.00	5.00	95.508
9	2160	0.75	4.00	93.696
10	3840	0.75	4.00	93.212
11	3000	0.33	4.00	94.000
12	3000	1.17	4.00	96.301
13	3000	0.75	2.32	95.424
14	3000	0.75	5.68	94.834
15	3000	0.75	4.00	96.451
16	3000	0.75	4.00	96.395
17	3000	0.75	4.00	96.336
18	3000	0.75	4.00	96.358
19	3000	0.75	4.00	96.450
20	3000	0.75	4.00	96.493

Note: A is the rotor speed, B is the KOH concentration, C is the flow rate, and EE is the fatty acid ethyl ester.

Table 3. Coefficient of predictive RSM model.

Coefficient	Value	*P*-Value
β_0	96.4070	0.000
B_1	-0.1437	0.003
B_2	0.6793	0.000
B_3	-0.1581	0.002
B_4	-1.0016	0.000
B_5	-0.4018	0.000
B_6	-0.4094	0.000
B_7	0.4919	0.000
B_8	-1.4439	0.000
B_9	1.4431	0.000

Note: The R^2 is 0.9969, and the $R^2_{adjusted}$ is 0.9941.

Table 4. The predictive RSM model.

Source	DOF	SS	MS	*F*-Value	*P*-Value
Reg.	9	59.161	6.574	356.44	0.000
R.E.	10	0.184	0.018		
LOF	5	0.166	0.033	5.15	0.167
Total	19	59.346			

Note: Reg. is the Regression, R.E. is the Residual Error, LOF is the lack of fit, DOF is the degree of freedom, SS is the sum of square, and MS is the mean of square.

3.3 Response Surface Plots

The contour plots illustrated the relationship between the EE content (C_{EE}) and the independent variables, namely (A) rotor speed, (B) KOH concentration [KOH], and (C) flow rate, as shown in Figure 2.

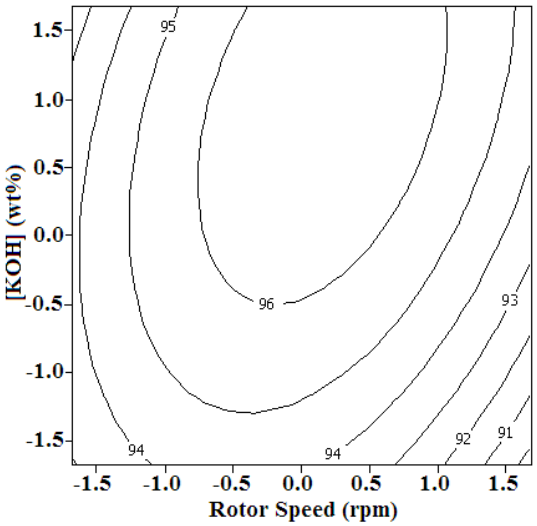

(a)

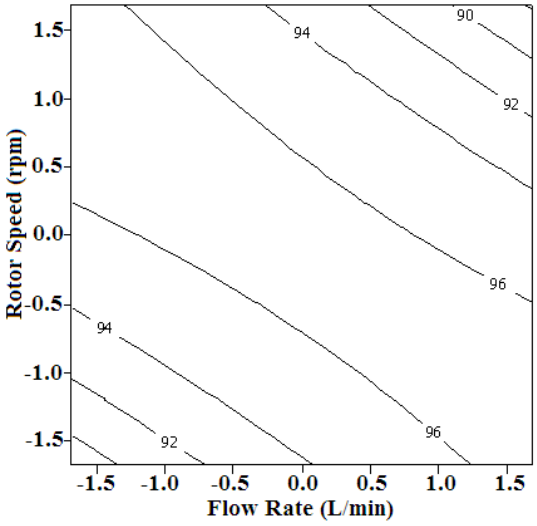

(b)

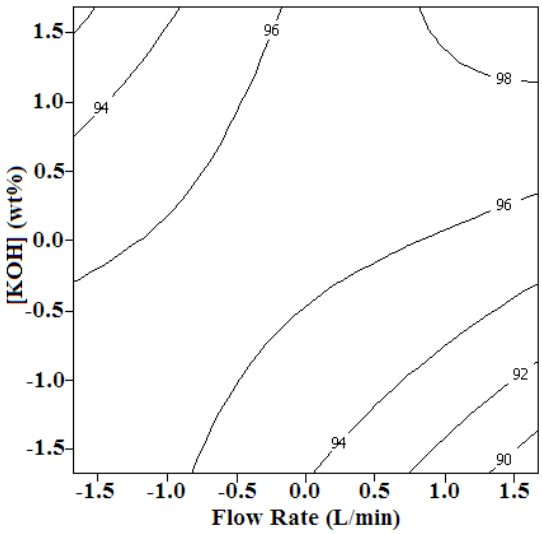

(c)

Fig. 2. Contour plots of the continuous ethyl ester production process (A), (B), and (C) affected by rotor speed and potassium hydroxide concentration [KOH], flow rate and rotor speed, flow rate and [KOH] in C_{EE}.

3.4 Optimal Conditions for Ethyl Ester

The test results of the RSM analysis in Minitab version16 were shown in Table 2. Equation 12 and the coefficients in Table 3 were integrated into the regression model equation for predicting the optimal conditions of predictive codes A, B, C, and C_{EE}.

The RSM model predicted optimal conditions of 3000 rpm rotor speed, 1.170 wt% [KOH], and 5.680 L/min flow rate and showed a C_{EE} of 98.84 wt%. The optimal conditions were verified by three repeats, showing an average C_{EE} of 98.11 wt%.

Reference [32] showed a predicted C_{ME} of 97.30 wt% with optimal conditions of 2907 rpm rotor speed, 1.106 wt% KOH, and 2.134 L/min flow rate. Three repeat experiments resulted in an average C_{ME} of 97.16 wt%.

3.5 Temperature and Pressure

Table 5 showed that the initial inlet temperature for EE and ME production was in the range of 311.45-311.95 K. After 30 s of start-up, the reference temperature (T_{REF}) at X_1 quickly rose by 0.2-0.3 K affecting the increase in vapor pressure (P_V). The alcohol vaporization at X_1 led to a decrease in T_{REF} at the X_2 point by 0.5-0.6 K. The flow of reactants from X_2 through X_3 increased $T_{REF\ (EE)}$ by 0.7 K, higher than $T_{REF\ (ME)}$, which increased by only 0.4 K, but affected the change in P_V, $_{(TREF)}$ of ME higher than EE. At X_D, $T_{REF\ (EE)}$ still increased more than $T_{REF\ (ME)}$, but at a lower rate of increase, corresponding to the P_V caused by the flow of the products to the outside at higher pressure. The type of alcohol affects the change in P_V, $_{(TREF)}$. The change in $P_{V, (TREF)}$ depended directly on the $P_{V, alc}$. Since the boiling point of palm olein oil was higher than 493.15 K, the P_V from palm olein oil ($P_{V, (WCO)}$) was low, nearly close to zero, at T_{REF} below 312.55 K [35].

The internal geometry of the reactor, as shown in Figure 1, affected the flow characteristics in which a steady flow of reactant from the reactor inlet with a cross-sectional area A_U of 2.834×10^{-4}m^2 passing through a larger cross-sectional area $A_{1,\ 2,\ 3}$ of 1.479×10^{-3} m^2 affected the reduction of V_X. While in combination with V_Y, the rotor speed was V_R. Following Bernoulli's principle, one could describe the increase in velocity within the reactor affecting the increase in kinetic energy per unit volume and the decrease in pressure energy leading to a decrease in pressure decreased at X_1.

The spiral flow of viscous fluid passed from X_1 and was compressed to increase the pressure through X_2, which caused the pressure to rise. The rotor 27.6 A_F% could reduce the pressure again at X_3, while a further increase in P_V affected the continuous stimulation of HC, which then flowed out through X_D, as shown in Table 5.

3.6 Significant Parameters

3.6.1 Resultant velocity

Under optimal conditions, the comparison between ME and EE production illustrated that the velocity of the steady flow could be calculated by converting the flow rates of 2.134 and 5.680 L/min to the velocities of 0.126 and 0.344 m/s V_X at points $V_{U, D}$, 0.024 and 0.064 m/s V_X at points $X_{1, 2, 3}$, respectively. The rotation speed of 2907 and 3000 rpm could be additionally converted to V_Y at 15.243 and 15.731 m/s. The V_X and V_Y combined were 15.244 and 15.732 m/s for V_R, indicating rapid flow of the precursors on the surface around the rotor. Table 6 showed the V_R of increasing EE, which could be achieved by increasing the rotor speed and flow rate. These flow rates and rotor speeds resulted in the rotation of the precursor around the rotor at 681 revolutions per 14.06 s and 264 revolutions per 5.28 s, respectively, for EE production. Hence, the higher V_R of EE production resulted in fewer revolutions around the rotor, which increased the severity of flow and saved operation time.

Table 5. Temperature/vapor and operated pressure at 30 s.

Exp.	$T_{(Xi)}/P_{V(Xi)}/P_{abs\ (Xi)}$				
	X_U	X_1	X_2	X_3	X_D
ME	311.45	311.75	311.15	311.55	311.65
	0.24539	0.24888	0.24194	0.24655	0.24771
	1.11325	0.91325	1.01325	0.91325	1.01325
EE	311.95	312.15	311.65	312.35	312.55
	0.12620	0.12752	0.12424	0.12886	0.13021
	1.11325	0.91325	1.01325	0.91325	1.01325

Note: T is the temperature (K), P_V and P_{abs} are the vapor and absolute pressure (10^5N/m^2). X_U, X_1, X_2, X_3, and X_D are the reference points and are detailed in Figure 1.

Table 6. Effect of rotor speed and flow rate on resultant velocity.

Description	ME	EE
Resultant velocity (m/s)	15.244	15.732
Rotor speed (rpm)	2907	3000
Flow rate (L/min)	2.134	5.680

3.6.2 Cavitation Number

The variation of the cavitation number (σ) explained the opportunity of hydrodynamic cavitation. The variation of the strength level of HC increased when σ was less than 1. This condition was characterized in particular by the following: firstly, the limitation of using the lowest mixing ratio alcohol: oil ratio of 3:1 could be improved by the choice of using an alcohol type with a high vapor pressure that also produced a mixture with a high vapor pressure. Secondly, the advantage of using a 3:1 molar ratio alcohol: oil changed the mixing density of the reactant due to the use of a smaller amount of alcohol. Thirdly, the RSM model chose a high flow rate combined with a medium rotor speed to become a high resultant velocity, which was a significant parameter that directly affected the high resultant velocity squared.

A comparison of (a) ME production and (b) EE production revealed that the vapor pressure of (b) was lower than that of (a), as shown in Table 5. The (b) process set a higher resultant velocity than the (a) process, as shown in Table 6. The (b) process set a lower mixing density of 906 kg/m^3 than the (a) process of 911 kg/m^3, which was calculated using the total mass flow rate per total volume flow rate. All the aforementioned reasons affected the EE production process by generating HC at X_1, X_2, and X_3 with σ average of 0.732, as shown in Table 7, with severe HC closed to the ME production process with σ average of 0.662.

3.6.3 Reynolds Number

According to ISO 80000-11:2019, the Reynolds number (*Re*) represented the ratio of inertial forces to viscous forces. *Re* could be used to compare flow behavior of laminar flow when viscous forces dominated inertial forces or turbulent flow when inertial forces defeated viscous forces. *Re* was defined as depending on the increasing resultant velocity, density and the length of touching lines through which the fluid flowed, but was inversely proportional to the dynamic viscosity.

At X_1, the reactants were a nonhomogeneous mixture of WCO, alcohol and KOH. The chemical reactions were still not occurring at this point. Under optimal conditions, a comparison of (a) ME and (b) EE production in Table 6 revealed that (b) had a higher resultant velocity than (a) due to increase flow rate and rotor speed.

Both the mixed density and dynamic viscosity of (a) were greater than (b) due to the type of alcohol and the molar ratio of 3:1. The kinematic viscosity of the mixture was tested under EN ISO 3104 standard by testing the kinematic viscosity of the alcohol mixed with WCO and applying Equation 9 to convert to dynamic viscosity (μ) and found that (a) was higher than (b). As a result, (a) had a lower *Re* at X_1 than (b), both being turbulent, as shown in Table 8.

Table 7. The σ under optimal conditions.

Reference points	ME	EE
X_U	11997.441	1842.195
X_1	0.628	0.702
X_2	0.729	0.794
X_3	0.630	0.700
X_D	10582.925	1648.081

Table 8. The *Re* and μ under optimal conditions.

Description	ME	EE
Reynolds number at X_U	74.11	199.29
X_1	4267.90	4449.80
Dynamic viscosity (mPa·s)	29.285	28.828

Note: Dynamic viscosity was tested by the SICUBU. X_U and X_1 are reference points.

3.7 Performance

The comparison of ethyl and methyl ester production performance was shown in Table 9, where the mass balance method under steady flow was used and found that:

For ethyl ester production, the WCO mass flow rate was set at 4.450 kg/min. The ethanol flow rate was adjusted at 1:3 oil: ethanol molar ratio using potassium hydroxide at 1.170 wt% as a catalyst. It was possible to change the WCO to 4.360 kg/min of neat biodiesel.

For methyl ester production, the WCO mass flow rate was set at 1.704 kg/min. The ethanol flow rate was adjusted at 1:3 oil: ethanol molar ratio using potassium hydroxide at 1.106 wt% as a catalyst. It was possible to change the WCO to 1.667 kg/min of neat biodiesel.

The ethyl ester production performance showed that 100 kg of WCO could be converted to 97.98 kg of neat biodiesel, and 100 kg of neat biodiesel contained 98.11 kg of ethyl ester. The energy consumption to produce one kg of neat biodiesel was 4.59 W-h.

The performance of methyl ester production [32] showed a 97.83 wt% yield conversion and 97.16 wt% methyl ester content. *SEC* was 12.00 W-h/ kg.

3.8 Physicochemical Properties

The physicochemical properties of WCO and WCO ethyl ester were tested as shown in Table 10 and the following (standard) were determined: density at 15°C (EN ISO 12185), kinematic viscosity at 40°C (EN ISO 3104), sulfur content (EN ISO 20846), acid value (EN 14104), calorific value (EN ISO 1928), water content (EN ISO 12937), mono-, di- and triglycerides (EN 14105), ester content (EN 14103), and total glycerol as given by:

$$G_T = G_F + 0.255(MG) + 0.146(DG) + 0.103(TG) \quad (13)$$

where G_T is the total glycerol (wt%) and G_F, MG, DG, and TG are free glycerol, mono-, di- and triglycerides (wt%) [32].

Table 9. Performance, Retention time, and Ester content under optimal conditions.

Description	ME[A]	EE
ĖC (W-h/min)	20	20
$\dot{M}_{NB}$ (kg/min)	1.667	4.360
SEC (W-h/kg)	12.00	4.59
(W-h/L)	13.63	5.16
Yield conversion (wt%)	97.83	97.98
Retention Time (s)	14.06	5.28
Ester content (wt%)	97.16	98.11

Note: A citation [32] and all Ester contents were tested by SICUBU in accordance with EN 14103.

Table 10. Physicochemical properties.

Properties	WCO[B]	ME[A]	EE[B]	EN 14214
Density (kg/m^3) at 15°C	921.7	880.0	888.5	860-900
Kinematic viscosity (mm^2/s) at 40°C	51.24	3.52	4.99	3.50-5.00
Sulfur content (mg/kg)	10.5	10.0	9.9	10.0 max
Acid value (mg KOH/g)	2.13	0.45	0.39	0.50 max
Calorific value (MJ/kg)	39.06	41.05	41.74	NA
Water content (mg/kg)	300	200	160	500 max
Glycerides (wt%)				
Free glycerin	-	0.01	0.01	0.05 max
Mono-glycerides	0.10	0.32	0.30	0.80 max
Di-glycerides	3.47	0.05	0.07	0.20 max
Tri-glycerides	96.43	0.02	0.01	0.20 max
Total glycerol (wt%)	-	0.10	0.09	0.25 max
ME/EE comp. (wt%)				
Myristic acid, C14:0	0.98	0.96	0.97	NA
Palmitic acid, C16:0	38.52	37.11	37.50	NA
Stearic acid, C18:0	6.02	5.95	6.00	NA
Oleic acid, C18:1	44.57	43.99	44.42	NA
Linoleic acid, C18:2	9.91	9.15	9.22	NA
ME/EE content (wt%)	-	97.16	98.11	96.5 min

Note: NA= not available, A citation [32], and B was tested by the SICUBU.

4. DISCUSSION

High-performance BSRR was applied to improve the efficiency of ethyl ester production from WCO, using a continuous transesterification process with an ethanol-to-oil molar ratio of 3:1.The success factors for correcting the disadvantages of using ethanol in ethyl ester production and making good improvements include:

Applying a 3:1 ethanol-to-oil ratio by molar aided in increasing the density value and optimal dynamic viscosity of the reactants that were used to produce ethyl esters. This is consistent with basic chemical knowledge indicating that the density and viscosity of precursor will be increased at the low temperature (311.45-313.45K). All density and viscosity directly varied on the size of the ethanol molecular, the higher oil concentration by weight in precursor at the low molar ratio, and higher polarities condition of the hydroxyl group in ethanol increasing the intermolecular attraction.

Choosing the optimal high-value of rotor speed and flow rate increased the maximum resultant velocity.

All factors such as high density, optimal dynamic viscosity, and higher resultant velocity (V_R) resulted in increased Reynolds number (*Re*) and reduced cavitation number (σ).

Adding V_R directly affected the increase in *Re*, and increasing the squared value of V_R directly affected the reduction of σ by less than 1. These reasons led to inertial forces overcoming viscous forces and generating turbulence with severe hydrodynamic cavitation, which was a significant level. This method could be used to compensate for the limitations of low vapor pressure of ethanol at room temperature.

Improved performance increased yield conversion and high ethyl ester content. A higher yield conversion with high flow rate and medium rotor speed reduced specific energy consumption. The highest V_R decreased the retention time and directly reduced the reverse reaction.

This view compared favorably with the use of methanol in the production, affecting the ethyl ester production process to be completely successful at the lowest molar ratio.

5. CONCLUSION

The high-performance BSRR was equipped with a rotor of 27.6 A_F% and was applicable to the production of ethyl esters from WCO.

The RSM regression model predicted the optimal conditions as follows: 3000 rpm rotor speed, 1.170 wt% KOH, and 5.680 L/min flow rate, with an average ethyl ester content of 98.11 wt% over three-replicates, close to the predicted value of 98.84 wt%. The yield conversion from WCO to neat biodiesel of 97.98 wt% reduced 0.00741 kW-h/kg of specific energy consumption.

The improvement of the ethyl ester production was good by increasing the resultant velocity to 15.732 m/s, resulting in an increase of the Reynolds number to 4449.80 and a decreased of the cavitation number to 0.732. When compared with methyl ester production, it was found that ethyl ester production increased the resultant velocity by 3.2%, affecting an increase of the Reynolds number by 4.26% and the cavitation number by 10.6%, thus reducing the strength level of HC, but still allowing improved production and reduced *SEC* by 59.83%. Yield conversion and ester content were increased by 0.153% and 0.978%.

ACKNOWLEDGEMENT

The National Research Council of Thailand (NRCT) financially supported the research and innovation activities, grant no. N41D640022.

ABBREVIATION

AV	Acid value
BSRR	Bumpy surface rotor reactor
DG	Di-glycerides
EE	Ethyl ester
FFA	Free fatty acid
HC	Hydrodynamic cavitation
KOH	Potassium hydroxide
ME	Methyl ester
MG	Mono-glycerides
MS	Mechanical stirrer
MW_{FFA}	Molecular weight of FFA
MW_{WCO}	Molecular weight of WCO
MW	Microwave
SEC	Specific energy consumption
TG	Tri-glycerides
UC	Ultrasonic cavitation
WCO	Waste cooking oil
Y	Yield conversion

LIST OF SYMBOLS

A_F	Area fraction
σ	Cavitation number
ρ	Density
C_{EE}	Ethyl ester content
$\dot{E}C$	Energy consumption rate
G_F	Free glycerol
μ	Dynamic viscosity
D_H	hydraulic diameter
ν	Kinematic viscosity
C_{ME}	Methyl ester content
$\dot{M}_{NB}$	Mass flow rate of neat biodiesel
$\dot{M}_{WCO}$	Mass flow rate of WCO
Re	Reynolds number
T_{REF}	Reference temperature
V_R	Result velocity
G_T	Total glycerol
P_V	Vapor pressure

REFERENCES

[1] Makareviciene V. and P. Janulis. 2003. Environmental effect of rapeseed oil ethyl ester. *Renewable Energy* 28: 2395-2403.

[2] Mallika T. and P. Wittaya. 2019. Production of ethyl ester biodiesel from used cooking oil with ethanol and its quick glycerol-biodiesel layer separation using pure glycerol. *International Journal of GEOMATE* 17(61): 109-114.

[3] Vicente G., Martinez M., and Aracil J., 2007. Optimization of integrated biodiesel production. Part I. A study of biodiesel purity and yield. *Bioresource Technology* 98: 1724-1733.

[4] Silva W., Souza P., Shimato G.G., and Tubino M., 2015. Separation of the glycerol–biodiesel phase in an ethyl transesterification synthetic route using water. *Journal of the Brazilian Chemical Society* 26(9): 1745-1750.

[5] Olivera S.S., Ana V.V., and Vlada B.V., 2011. The production of biodiesel from vegetable oils by ethanolysis: current state and perspectives. *Fuel* 90: 3142-3155.

[6] Vicente G., Martinez M. and Aracil I., 2004. Integrated biodiesel production: a comparison of different homogeneous catalysts system. *Bioresource Technology* 92: 297-305.

[7] Lotero E., Liu Y., Lopez D.E., Suwannakarn K., Bruce D.A., and Goodwin Jr. J.G., 2005. Synthesis of biodiesel via acid catalysis. *Industrial & Engineering Chemistry Research* 44: 5353-5363.

[8] Kucek K.T., César-Oliveira M.A.F., Wilhelm H.M., and Ramos L.P., 2007. Ethanolysis of refined soybean oil assisted by sodium and potassium hydroxides. *Journal of the American Oil Chemists' Society* 84(4): 385-392.

[9] George A., Ypatia Z., Stamoulis S., and Stamatis K., 2009. Transesterification of vegetable oils with ethanol and characterization of the key fuel properties of ethyl esters. *Energies* 2: 362-376.

[10] Enweremadu C.C. and M.M. Mbarawa. 2009. The technical aspect of production and analysis of biodiesel from used cooking oil: a review. *Renewable and Sustainable Energy* 13: 2205-2224.

[11] Ahmad Farid M.A., Hassan M.A., Taufiq-Yap Y.H., Ibrahim M.L., Othman M.R., and Ali A.A.M., and Shirai Y., 2017. Production of methyl esters from waste cooking oil using a heterogeneous biomass-based catalyst. *Renewable Energy* 114: 638-643.

[12] Qiu Z., Zhao L., and Weatherley L., 2010. Process intensification technologies in continuous biodiesel production. *Chemical Engineering and Processing Process Intensification*. 49(4): 323–330.

[13] Veerachai L., Rattanachai P., Kornkanok A., and Kanit K., 2008. Microwave-assisted in continuous biodiesel production from waste frying palm oil and its performance in a 100 kW diesel generator. *Fuel Processing Technology* 89: 1330-1336.

[14] Kittiphoom S., Sukritthira R. and Chakrit T., 2010. Production of ethyl ester from esterified crude palm oil by microwave with dry washing by bleaching earth. *Applied Energy* 87: 2356-2359.

[15] Kumar D., Kumar G., and Singh P.C.P., 2010. Fast easy ethanolysis of coconut oil for biodiesel production assisted by ultrasonication. *Ultrasonic Sonochemistry* 17: 555-9

[16] Hanh H.D., Dong N.T., Okitsu K., Nishimura R., and Maeda Y., 2009. Biodiesel production through transesterification of triolein with various alcohols in an ultrasonic field. *Renewable Energy* 34: 766-8

[17] Gogate P.R. and A.B. Pandit. 2021. Hydrodynamic cavitation reactors: a state-of-the-art review. *Reviews in Chemical Engineering* 17: 1–85.

[18] Saharan V.K., Rizwani M.A., Malani A.A., and Pandit A.B., 2013. Effect of the geometry of hydrodynamically cavitating device on the degradation of orange-G. *Ultrasonics Sonochemistry* 20(1): 345–353.

[19] Patil A.D., Baral S.S., Dhanke P.B., and Dharasker S.A., 2022. Cleaner production of catalytic thumba methyl ester (Biodiesel) from thumba seed oil (Citrullus Colocyntis) using TiO_2 nanoparticles under intensified hydrodynamic cavitation. *Fuel* 313: 123021.

[20] Paul E.L., Atiemo-Obeng V.A., and Kresta S.M., 2004. *Handbook of industrial mixing: science and practice*. Hoboken: Wiley-Interscience.

[21] Alhashan T., Addali A., and Teixeira J.A., 2018. Experimental investigation of the influences of different liquid types on acoustic emission energy levels during the bubble formation process. *International Journal of Energy and Environmental Engineering* 9: 13–20.

[22] Husin S., 2011. *An experimental investigation into the correlation between acoustic emission (AE) and bubble dynamics*. Bedford: Cranfield University.

[23] Naveen N.S. and A.N. Los. 2004. *Characterization of liquids using gas bubbles*. United States: Patent Application Publication.

[24] Weninger K.R., Camera C.G., and Putterman S.J., 1999. Energy focusing in a converging fluid flow: implications for sonoluminescence. *Physical Review Letters* 83(10): 2081-2084.

[25] Brennen C.E., 1995. *Cavitation and bubble dynamics*. Oxford: Oxford University Press.

[26] Joelianingsih H., Maeda S., Hagiwara H., Nabetani Y., and Soerawidjaya S.T.H., 2008. Biodiesel fuels from palm oil via the non-catalytic transesterification in a bubble column reactor at atmospheric pressure: a kinetic study. *Renewable Energy* 33: 1629–1636.

[27] Chuah L.F., Yusup S., Aziz A.R.A., Bokhari A., and Abdullah M.Z., 2016. Cleaner production of methyl ester using waste cooking oil derived from palm olein using a hydrodynamic cavitation reactor. *Journal of Cleaner Production* 112: 4505–4514.

[28] Petkovšek M., Zupanc M., Dular M., Kosjek T., Heath E., Kompare B., and Sirok B., 2013. Rotation generator of hydrodynamic cavitation for

water treatment. *Separation and Purification Technology* 118: 415–423.

[29] Badve M., Gogate P., Pandit A., and Csoka L., 2013. Hydrodynamic cavitation as a novel approach for wastewater treatment in wood finishing industry. *Separation and Purification Technology* 106: 15–21.

[30] Samani B.H., Behruzian M., Najafi G., Fayyazi E., Ghobadian B., Behruzian A., Mofijur M., Mazlan M., and Yue J., 2021. The rotor-stator type hydrodynamic cavitation reactor approach for enhanced biodiesel fuel production. *Fuel* 283: 118821.

[31] Ye M.O., Gumpon P., and Krit S., 2021. Two-stage continuous production process for fatty acid methyl ester from high FFA crude palm oil using rotor-stator hydrocavitation. *Ultrasonics Sonochemistry* 73: 105529.

[32] Wuttisan K. and T. Prachasanti. 2022. Optimization of continuous FAME production in high-performance bumpy surface rotor reactor under theoretical molar ratio by response surface methodology. *Journal of Oleo Science* 71(11): 1591-1603.

[33] Mingming G., Chuanyu S., Guangjian Z., Olivier C.D., and Dixia F., 2022. Combined suppression effects on hydrodynamic cavitation performance in venturi-type reactor for process intensification. *Ultrasonic Sonochemistry* 86: 106035.

[34] Ambrose D., Sprake C.H.S. and Townsend R., 1975. Thermodynamic properties of organic oxygen compounds. XXXVII. Vapor pressures of methanol, ethanol, pentan-1-ol, and octan-1-ol from the normal boiling temperature to the critical temperature. *Journal of Chemical Thermodynamics* 7(2): 185-190.

[35] Jamoussi B., Jablaoui C., Hajri A.K., Chakroun R., Al-Mur B., and Allaf K., 2022. Thermomechanical Autovaporization (MFA) as a deodorization process of palm oil. *Foods* 11(24): 3952.